



Robust blood vessel detection with image enhancement using relative intensity order transformation and deep learning

Chandrakala Kuruba ^{*}, N.P. Gopalan

National Institute of Technology, Tiruchirappalli, Tamil Nadu, India



ARTICLE INFO

Keywords:

Diabetic retinopathy
Segmentation
Blood vessel
Bio medical image processing
Relative intensity transformation

ABSTRACT

Background: An eye-related diabetic microvascular condition is called diabetic retinopathy (DR). Injury to the retinal blood vessels, one of the main causes of blindness worldwide, is a severe public health problem. The vessel growth within the retina, and the likelihood of change in the estimation of retinal veins are important for understanding the stage of diabetic retinopathy. Segmenting retinal blood vessels is necessary to see the changes. Purpose: To develop a framework to improve the quality of the segmentation findings over diabetic retinal datasets.

Method: Deep learning-based approaches now show outstanding performance on blood vessel segmentation. However, the majority of them concentrate on designing powerful deep learning architectures rather than capturing the underlying curvilinear structure feature (e.g., the curvilinear structure is darker than the background). In this paper, a robust blood vessel segmentation technique is proposed that captures the characteristics of the blood vessel using relative intensity order transformations (RIOT) and statistical edge-based features. The RIOT extract the thick vessels considering 16 pixels on the horizontal and vertical directions, and the statistical edge features are used to extract the thin blood vessels. The proposed method balances the extraction of thin and thick blood vessels providing robust blood vessel segmentation insensitive to contrast variance in images.

Results: The proposed method is validated on the DRIVE, CHASEDB1 and STARE datasets. The proposed model achieved a segmentation accuracy of 96% on the DRIVE dataset, 99% on CHASEDB1 dataset and 87% on STARE dataset.

Conclusions: The paper has presented a framework that is contrast invariant in extracting the thick blood vessels using RIOT and thin vessels using statistical edge features and proposed framework has outperformed the existing models.

1. Introduction

The international Diabetic retinopathy (DR) scale classifies DR into four categories, depending on the risk of progression: mild non-proliferative DR (NPDR), moderate NPDR, severe NPDR, or PDR [1–4]. At the NPDR stages, lesions such as microaneurysms (MAs), haemorrhages (HEM), hard exudates (EX), and soft exudates were present [5]. The PDR stage of DR completely depends on the features of the retinal blood vessels. These features assist in identifying the DR stage as being in PR or NPDR. In the PDR stage, new blood vessels get created in the retina, occurring at the vitreoretinal interface (namely, neovascularization). These tiny vessels form during neovascularization but are only detected in the proliferative stage. Early detection of PDR stages is critical because they cause blindness in humans.

DR detection in blood vessels frequently depends on extracting the curvilinear shapes. Blood vessel segmentation has a variety of unique

challenges when compared to conventional object segmentation [6]: (1) thin, lengthy, and twisted shapes; (2) low contrast between blood vessels and the retinal background image; (3) no homogeneity in contrast; and (4) a wide range of image appearances. Traditional curvilinear object segmentation techniques [7] mainly focus on developing specially engineered features in order to address these issues. They often employ filters or specific morphological techniques in order to extract features from images. These feature-based techniques often necessitate careful parameter adjustment and are difficult to manage across a large range of complex blood vessel structures [8].

Teresa et al.'s put out a heuristic-based data augmentation strategy that would create structures that are similar to neo-vessels (NV) to make up for the absence of PDR cases in DR-labeled datasets. A thorough understanding of the specific position and form of these structures

* Corresponding author.

E-mail address: chandrakala.kuruba25@gmail.com (C. Kuruba).

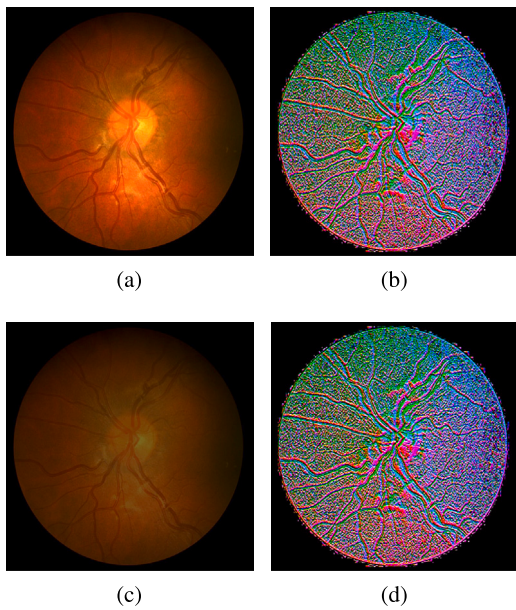


Fig. 1. Contrast invariant robust blood vessel segmentation.

forms the foundation of the proposed neo-vessel synthesis method. Deep neural networks can be used to increase their training sets by creating and inserting NVs into already-existing retinal images [9]. For the purpose of creating high-resolution fundus images, Yi Zhou et al. presented the diabetic retinopathy generative adversarial network (DRGAN). To control the managed synthesis grading severity, the adaptive grading mechanism defined by latent gradients was used [10].

Many DR detection algorithms consider the publicly available datasets containing real world cases for evaluation, comparison, and validating the algorithms. As they do not consider all the parameter ranges in the datasets, the actual validity of the algorithms is not known. In this study, DR data is simulated using computer vision for normal and NPDR phases (mild, moderate, and severe), with differences in retinal and image characteristics that indicate DR severity level over the complete range of parameters.

Recent algorithms [11–18] use deep learning [19,20] to segment curvilinear objects and significantly outperform previous approaches. To enhance the performance of segmentation, these techniques mostly concentrate on building various network designs or loss functions. The most advanced algorithms have great accuracy with in the same dataset, but are not robust with varied contrast images.

This suggests that it is still difficult to develop robust blood vessels segmentation techniques. It is essential to come up with a reliable approach to extract the features of blood vessel structures. This work aims to address the aforementioned problem and focuses on enhancing the robustness of segmenting the blood vessels with the use of deep learning. The Relative Intensity Order Transformation (RIOT), is designed to extract the blood vessel structure and invariant to the image contrast, is a novel image transformation that is introduced instead of working directly on the original image.

In the paper, the idea here is to compare the current pixel with the neighboring pixel intensity order using euclidean distance. Here, two order transforms in horizontal and vertical directions within a specific distance are used to generate a two-channel output. Also, edge based statistical features are generated and are combined with RIOT image to form three-channel image. This captures the fundamental properties of the blood vessel structure without relying on the absolute intensity value as shown in Fig. 1.

Any deep learning-based technique can use RIOT by just plugging in a different input. RIOT processed images are used as the input dataset

to the latest IterNet deep learning network and perform experiments on three datasets: DRIVE [21], STARE [22], and CHASEDB1 [23], in order to produce a potent sequence that can efficiently extract the blood vessels. This approach is very effective in capturing the characteristics of the blood vessels and enhancing the robustness of existing methods.

The following is the paper's primary contribution:

- An enhancement to the novel image transformation technique that captures the inherent properties of blood vessels in diabetic retinopathy images and is insensitive to changes in image contrast.
- Multinomial sub histogram approach to enhance the image for highlighting the thick blood vessels.
- A robust approach to capture the characteristics of the blood vessel using relative intensity order transformations in the horizontal & vertical directions and statistical edge-based features for extracting thin blood vessels.
- The use of RIOT as an input to a deep learning-based technique enables the model to express better generalization for the extraction of blood vessels.

Further, the paper is organized as follows: Section 2 discusses about preliminaries and the related works. Section 3 encompasses details regarding the dataset and proposed method. Section 4 is devoted to experimental results and discussion. Finally, Section 5 is the concluding section.

2. Related work

The goal of the work is to assist clinical professionals by offering this model as a pre-test that reduces testing time and costs in cases of PDR retinopathy. The work's goal is to create an automated diagnosis tool that can quickly detect new aberrant blood vessels from the retinal fundus.

2.1. Diabetic impact on blood vessels

Diabetes develops as a result of oxidative stress, which is caused by an imbalance between the cellular antioxidant system and reactive oxygen species generation(antioxidant mechanism) under hyperglycemic circumstances [24]. Due to the loss of neuronal and pericyte cells due to the rising oxidative stress, capillaries become clogged. The microvascular structure of the retina is distorted and deformed due to blocked capillaries and an increase in blood vessels [25] causing severe PDR. More bleeding will impair vision and lead to blindness. The new blood cells produce the scar tissue. The term NPDR is an early stage that refers to blood vessels swell and sometimes bulge or balloon (aneurysm) during this stage. This condition is known as macular edema [24]. The blood vessels aneurysm, abnormal growth, Hemorrhages are shown in Fig. 2

2.2. Segmentation of blood vessels

Early detection of blood vessels plays a crucial place in diagnosing the blood pressure, rapture of vessels and the diabetic stage in which the patient is present. The extraction of blood vessels from retinal images were always challenging due to the poor contrast of the nerves, similar shape appearing at random locations of eye. Through accurate segmentation of the blood vessels, automated segmentation of the retinal blood vessels is critical for measuring geometrical features like angle, reducing the number of incorrectly identified lesions during DR monitoring systems, and capturing other eye related diseases. For instance, they demonstrate that patients with hypertension had a decreased angle between the two offspring arterioles. Therefore, it is essential to precisely segment retinal blood arteries in order to identify retinal structures like optic disks and to detect various disorders like high blood pressure, strokes, and other comparable conditions like macular degeneration.

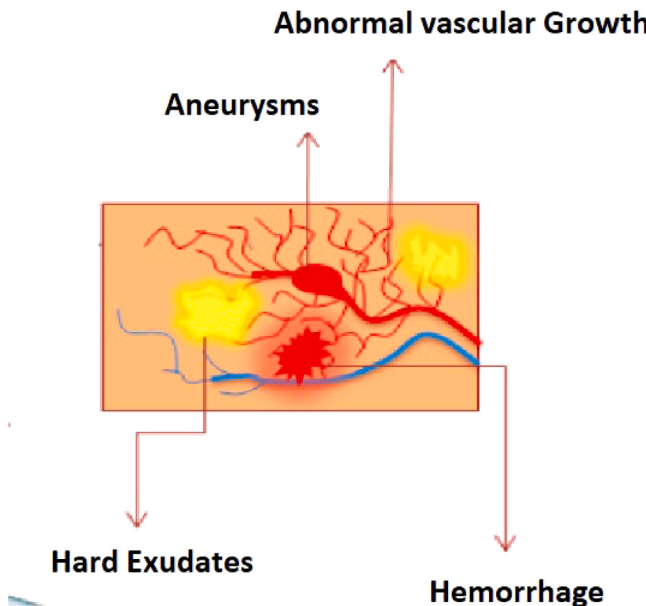


Fig. 2. Diabetic Impact on blood vessels.

2.3. Deep learning methods for blood vessel segmentation

Zhang et al. [26–30] proposed blood vessel segmentation using neural network and ensemble models, but the models were not able to segment thin blood vessels and validation on pathological images is not performed. Guo et al. [31] proposed blood vessel segmentation using multi level and multi scale convolution neural network (CNN) with short connections in forward and backward. These connection enhance the segmentation with the data available with high level to low level and vice versa. Many CNN based models were developed for vessel segmentation. The method was able to segment the tiny vessels as well. A method that balances the thick and tiny vessel segmentation is proposed in paper [32]. Many reviews were proposed on deep learning methods for blood vessel segmentation [33–36]. Semi supervised model U-Net is proposed to extract vessels and label them [37]. To extract well-defined vessel features from the global feature space, a two-stage vessel extraction framework is devised using VGG16 [38]. Shi et al. [39] proposed local intensity transformation to detect the blood vessel in low contrast images as well. Many feature extraction and image enhancement based methods were also proposed in literature [40,41] to extract the blood vessels using deep learning. However, the models need to be robust in varied contrast and less time complexity in extracting the tissues.

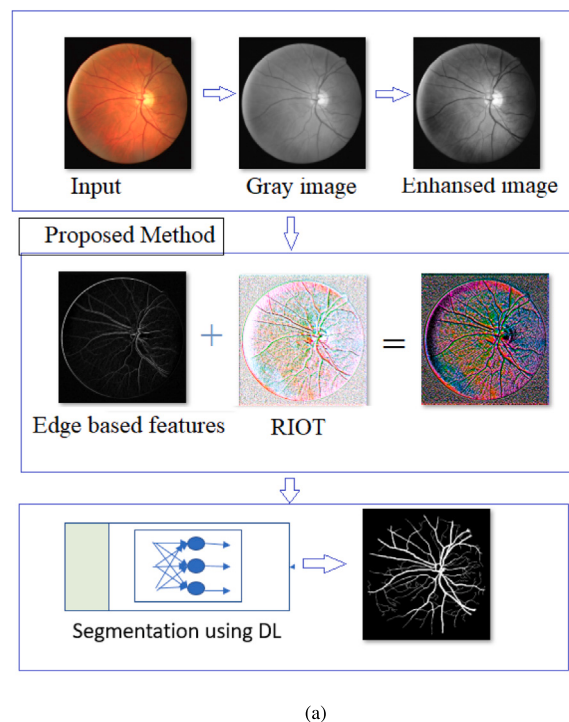
While working on the improvement of deep learning models, a number of factors, such as data augmentation, model development, and training are considered for vessel segmentation.

2.3.1. Imbalance vessels

Pixel-wise loss functions place a cap on the precision of thin vessel segmentation by deep learning models because of the disparity in pixel numbers between thick and thin vessels in fundus images. A three stage model for identifying thick, thin and fusion vessels is used to detect blood vessels. The accuracy of the deep learning models can be improved if the prior knowledge on the vessel structure is available and the balance between the vessels.

2.3.2. Robust learning

Robust blood vessel segmentation is another area where the deep learning models can improve. [39] proposed a local intensity order transformation to extract blood vessel in different contrast. Rather than using absolute statistical pixel ordering, using relative ordering results in performance accuracy.



(a)

Fig. 3. Proposed method of blood vessel extraction.

3. Proposed methodology

In this paper a novel methodology for segmenting blood vessels in diabetic fundus images is presented. For this purpose DRIVE, STARE and CHASEDB1 datasets are used. The image qualities are enhanced by using multinomial sub image histogram equalization and statistical edge based feature extraction and relative intensity transformation are performed.

The image is first converted to gray scale and then multinomial sub histogram enhancement is performed. The edge based statistical features generating one channel image and relative intensity order transformation to generate a two channel image are combined to form a three channel image. Finally, IterNet based on U-Net models is used to extract the blood vessels from the enhanced images obtained with prior processes. The performance metrics used to evaluate the proposed methodology are accuracy, specificity, sensitivity, precision, F1-score, and area under the curve. The flowchart of the proposed methodology is depicted in Fig. 3.

3.1. Preprocessing and data augmentation

A preprocessing technique called multinomial sub histogram image enhancement is used to enhance the image in order to address the problem of robust learning in presence of contrast in variance. In varied contrast level as well the model should effectively detect the blood vessels. Also, relative intensity order transformation assist in extracting features that assist in generalized feature extraction helping in robust learning. Many authors considered generative methods to augment the data, as existing methods failed to consider tiny vessels and result in mis-segmentation [42,43]. GANs are capable of producing a high number of samples, but it is challenging for them to guarantee the consistency of the data distribution between the new data and the actual fundus images. For instance, it is impossible to accurately mimic changes in the depth of blood vessels. Hence, in the work the basic data augmentation techniques like rotation, shearing, flipping, zooming and cropping are used.

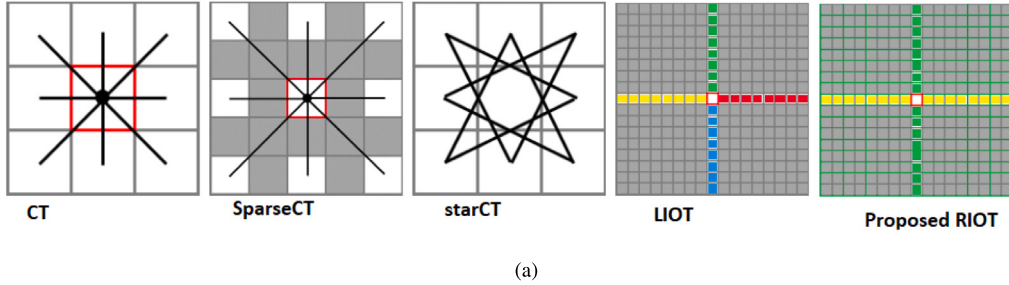


Fig. 4. Different local intensity transformations.

3.1.1. Multinomial sub histogram enhancement

The procedure known as “Histogram Equalization” (HE) equalizes the image histogram for image enhancement. In order to retain an image’s visual quality while boosting local contrast, histogram equalization enhances the brightness locally and improves the contrast. Different histogram base image enhancement methods exist in literature name Contrast-limited adaptive histogram equalization (CLAHE), Exposure based sub image histogram equalization(ESIHE), Recursive exposure based sub image histogram equalization (R-ESIHE), Median-Mean Based Sub-Image-Clipped Histogram Equalization (MMSICHE), Brightness Preserving Dynamic Fuzzy Histogram Equalization (BDPHE), Adaptive Gamma Correction With Weighting Distribution (AGCWD) and are reviewed in paper [44]. The authors have proposed a method based on central moment and multinomial sub image histogram equalization using clipping. In this approach, the multinomial curvature fitting function is used to process the image histogram and reduce the count of pixels needed to represent each intensity value. Using the least of the sum of squared residuals, the count is reduced. The calculated data is then smoothed via re-sampling. To limit the over-enhancement rate, the central moment is used on the resampled data to compute the threshold required for clipping the histogram. Two sub-histograms are evenly distributed within the histogram. By using a transfer function to equalize the sub histograms, the sub images are combined and produced as enhanced image. The final enhanced image is produced by removing the atmospheric haze in the image by estimating atmospheric light using a dark channel prior with the estimated transmission map. The same approach is employed to enhance the input image.

3.1.2. Relative intensity order transformation

Many local transformation methods based on Census transformation (CT) namely MeanCT, SparseCT, GeneralizedCT, SymmetricCT, StarCT and LIOT are available in literature [39] and few are shown in Fig. 4. LIOT is very effective in extracting the generalized features that can effectively assist the deep learning models. This generates four channel image that is fed to segmentation network. To add more effectiveness to the model, the edge detection filters are used to generate a channel, and the modified LIOT is used to generate two channel image rather than four channel image. Finally the three channel image with edge features and two channel images of modified LIOT is fed to the segmentation network as shown in Fig. 5. The proposed RIOT consider the relative values rather than absolute value and as a result, this is a more robust for extracting blood vessels from images in presence of varying contrasts.

For every pixel p in the image, we compare 8 pixels values above and 8 pixels below, i.e 16 pixels to produce vertical channel and 16 pixels horizontally, left 8 pixels and right 8 pixels to produce horizontal channel. The pixel is compared with 16 neighboring pixels $\{n_s^i, i = -8, -7, \dots, 7, 8\}$, $s = \{v, h\}$, v is vertical and h is the horizontal euclidean distance in perpendicular to p . The corresponding two channel output image is calculated with Eq. (1).

$$f'_s(p) = \sum_{i=-8}^8 [f(p) > f(n_s^i)] \times 2^{i-1} \quad (1)$$

where $[f(p) > f(n_s^i)]$ is 1 if the value $f(p)$ is larger than $f(n_s^i)$, otherwise 0. As per Eq. (1), the proposed RIOT rely on the relativity order of neighborhood intensity, detecting the darker values and is robust to change in contrast of images. Hence, providing a better version for generalized detection of blood vessels.

3.1.3. Segmentation network architecture

The proposed approach is not intended to build a strong network that outperforms other approaches because the main objective of the model is to increase the robustness with the current deep learning methods. The IterNet’s input channel is modified to read the image provided by enhanced image. we applied the enhanced image with edge and RIOT to the most recent version of IterNet [41]. Iternet is a three-mini U-Net combination that uses U-Net as the foundation module and is an encoder-decoder model similar to U-Net. With fewer parameters than U-Net, each tiny U-Net makes use of the feature maps from its predecessor module.

3.2. Training objective

The network shown in the section is used to segment the blood vessels. The loss used in IterNet is used for the same. The optimization of the segmentation network parameters is performed by calculating the loss of sigmoid cross entropy given in Eq. (2).

$$L = \sum (-f_i \log(p_{(f_i)}) - (1 - f_i) \log(1 - p_{(f_i)})) \quad (2)$$

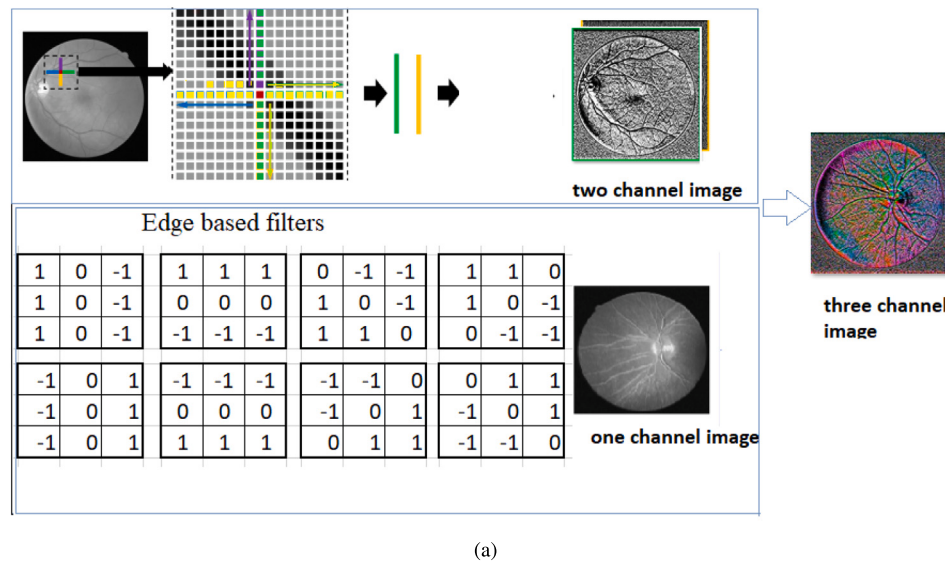
Here, f_i represents 0 or 1 indicating the pixel belonging to the ground truth image, $p_{(f_i)}$ is the probability of the intensity of the pixel i in the input image. The images are converted to gray scale and the multinomial image enhanced image with 3 channel edge and relative intensity transformation features is fed to the network while testing to produce the final result.

4. Experimental results and discussion

On three commonly used datasets—DRIVE [45], STARE [22] and CHASEDB1 [46] the assessment of the suggested technique is performed. In Section 4.1, a brief summary of these data-sets and the evaluation metrics used are provided. Then, in Section 4.2, certain implementation details are illustrated. Two different sorts of experiment evaluations are performed to show the proposed RIOT’s robustness: (1) Section 4.3 analysis to show that the proposed edge and RIOT does not materially impair the performance of the original images; (2) An evaluation of images to demonstrate that RIOT is more resistant to contrast variance.

4.1. Datasets and evaluation metrics

Numerous databases contain retinal images, particularly for DR, but we discovered that three of them are the most comprehensive and regularly cited in the literature. These datasets are the DRIVE, STARE and CHASEDB1 [45]. The DRIVE dataset was developed to facilitate



(a)

Fig. 5. Proposed relative local intensity transformation combined with edge features.

Table 1
Datasets used for simulation.

Dimension	Dataset	Number of images	Test images	Train images	Image size
2D	DRIVE	40	20	20	565 × 584
2D	STARE	20	10	10	700 × 605
2D	CHASEDB1	10	8	20	999 × 960

comparative study on retinal blood vessel segmentation and identification of morphological retinal blood vessel parameters, including length, width, texture, branch pattern, and angle, which are often used to diagnose, screen for, treat for, and evaluate DR. [21]. The DRIVE dataset contains 20 training images and 20 testing images. The STARE has 20 color fundus images, of which 10 are training retinal images and 10 are testing. The CHASEDB1, a dataset of colored fundus DR images created for research, is the third example. The dataset contains 20 training images and 8 test images. The Table 1 shows the datasets and their sizes. Different image resolutions can result in varying thickness in images featuring curved objects like blood vessels. To address such a scale disparity, the size of the field of view (FOV) and image size, each retinal image is adjusted to a comparable scale. The DRIVE dataset size remains constant while CHASEDB1 images are resized from 999 × 960 to 584 × 561 and STARE images from 700 × 605 to 554 × 479. Both the reference methods and the suggested method employ these size values.

Segmentation accuracy (seg_acc), sensitivity, specificity, precision, dice_coefficients and F1-score are used as performance measurements to quantitatively compare the segmentation results with the ground truth. The true positives, true negatives, false positives, false negatives are computed to measure the SA, SEN, SPE, AUC and F1-score.

4.2. Implementation details

The data augmentation techniques are required for removing noise from fundus images and enlarging the retinal dataset at various sizes. Here is a list of the main data augmentation techniques that are used in the proposed method.

- Rotation: Images were randomly rotated between -180 and 180 degrees.
- Shearing: Sheared with an arbitrary angle between -0.1 and 0.1 degrees.
- Image flipping: Both the horizontal and vertical axes of images were flipped.
- Zoom: Images were arbitrarily zoomed between 0.8 and 1.2 .

- Cropping: Images were arbitrarily reduced to 128×128 of their original size.

Our major goal is to check for robustness of the method invariant to contrast not to build a robust network that outperforms other methods. Here, RIOT is employed with the most recent IterNet [41]. According to this model the network is trained using cross-entropy loss over 200 epochs using a batch size of 32. Adam optimizer with a learning rate of 0.001 is used to optimize the network. The RIOT is implemented with a stride of 8 with overlapping in images.

4.3. Experimental results

The first experiment is performed to analyze the enhancement of the images. The input image converted to gray scale is enhanced with multinomial sub histogram clip enhancement. Further, the edge features extracted and the RIOT of the images are shown in Fig. 6.

From Fig. 6 it can be seen that edge based features and the two channel relative intensity order transform retains the vessel details in spite of varied contrast in different input images. Further, the experiment is performed to verify the extraction of blood vessels from the images. Different images from the three datasets are considered for this experiment. In Fig. 7 the first row shows the DRIVE 04_test image and its RIOT image, ground truth, extracted using proposed method; and Second row the same sequences for DRIVE 05_training image; third row: same sequences for STARE 001 image ; fourth row: same sequences for CHASE image001 image; fifth row: same sequences CHASE image006. Visually, the segmentation of blood vessels are effectively extracted with the proposed method and does not materially impair the performance of the original images. Fig. 8 shows the zoomed images of test04 and training05 images, in comparison with IterNet [41], LIOT [39]. Visually, the algorithm effectively extracts the blood vessels in comparison with the latest methods. The proposed method shows the balance of the small vessels and the thick vessels in extracting them.

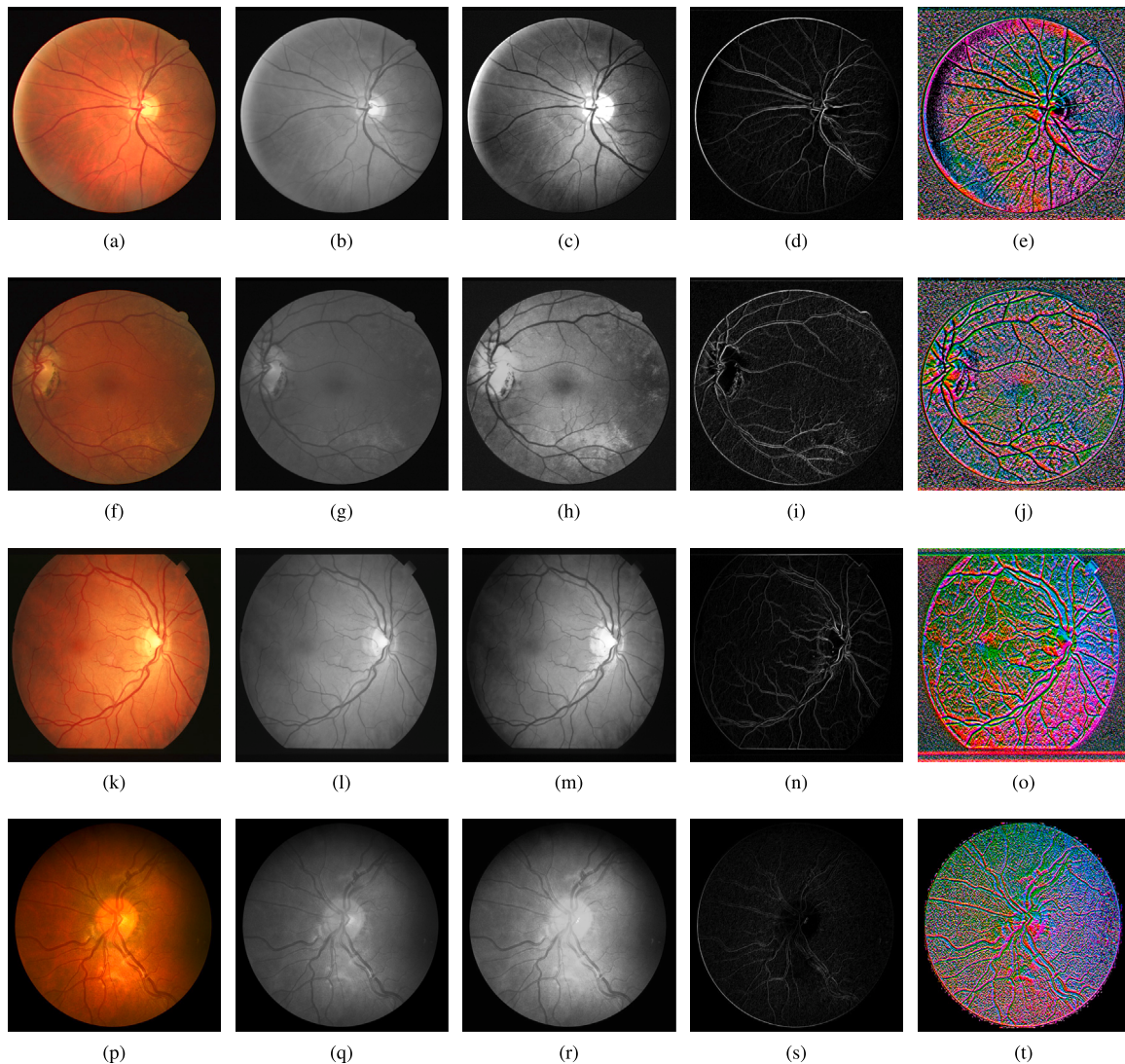


Fig. 6. First Column: DRIVE test04, DRIVE train 26, STARE train34 and CHASEDB1 06 Images; Second column: Gray images; Third column: Enhanced images; Fourth column: Edge features; Fifth column: 3 channel RIOT images.

The proposed method effectively handles the challenges of deep learning, for lack of datasets using augmentation technique, balancing the thin and thick vessels using edge and relative intensity order transformation and robust extraction of vessels that are invariant to contrast of images. The seg_acc, sensitivity, specificity, precision, dice_coefficient and F1score of the proposed method are shown in **Table 2**. The table has shown the measures for individual images of DRIVE, CHASEDB1 and STARE datasets and also average values of the datasets. The performance of the proposed model on DRIVE dataset resulted in 96% accuracy, CHASEDB1 dataset with 99% and STARE dataset with 87%. The precision, sensitivity, specificity, dice coefficient and f1 score are showing good performance on DRIVE and CHASEDB1 datasets, while not that effective on STARE dataset.

The experiment is further compared with the different transformation used in extracting the blood vessels namely the baseline, census transform, LIOT, RIOT and RIOT combined with edge features. The results in the **Table 3** demonstrate that the proposed method outperforms the existing methods for DRIVE and CHASEDB1.

Further, the performance evaluation of the proposed model is compared with other latest models namely IterNet [41] and LIOT [39]. In comparison with these models presented in table **Table 4**, the performance of the proposed model is not degraded and it has shown equal of good measure when compared to LIOT. For DRIVE and CHASEDB1

dataset the proposed method outperformed the other two models, while for the STARE dataset, sensitivity was more when compared to other models and not effective in case of accuracy but shown good performance than IterNet.

5. Conclusion

The focus of this research is to enhance the robustness of existing deep learning-based blood vessel segmentation techniques that are invariant to contrast. A relative intensity order transformation is used to identify the local relativity among the pixels along with statistical edge-based features. With this approach, the balancing between the thin blood vessels and thick blood vessels is retained, which assists in effective segmentation. Also, in order to address the challenge of data imbalance, augmentation techniques are used to enhance the dataset. The IterNet deep learning model was used to train the transformed images obtained with relative intensity order transformation and statistical edge features in the proposed algorithm. The proposed model is an alternative attempt to make a robust blood vessel segmentation algorithm, i.e., one that is invariant to contrast like LIOT. Further, for reliable blood vessel segmentation, more complex algorithms deserve further study as the proposed model was not effective on the STARE dataset.

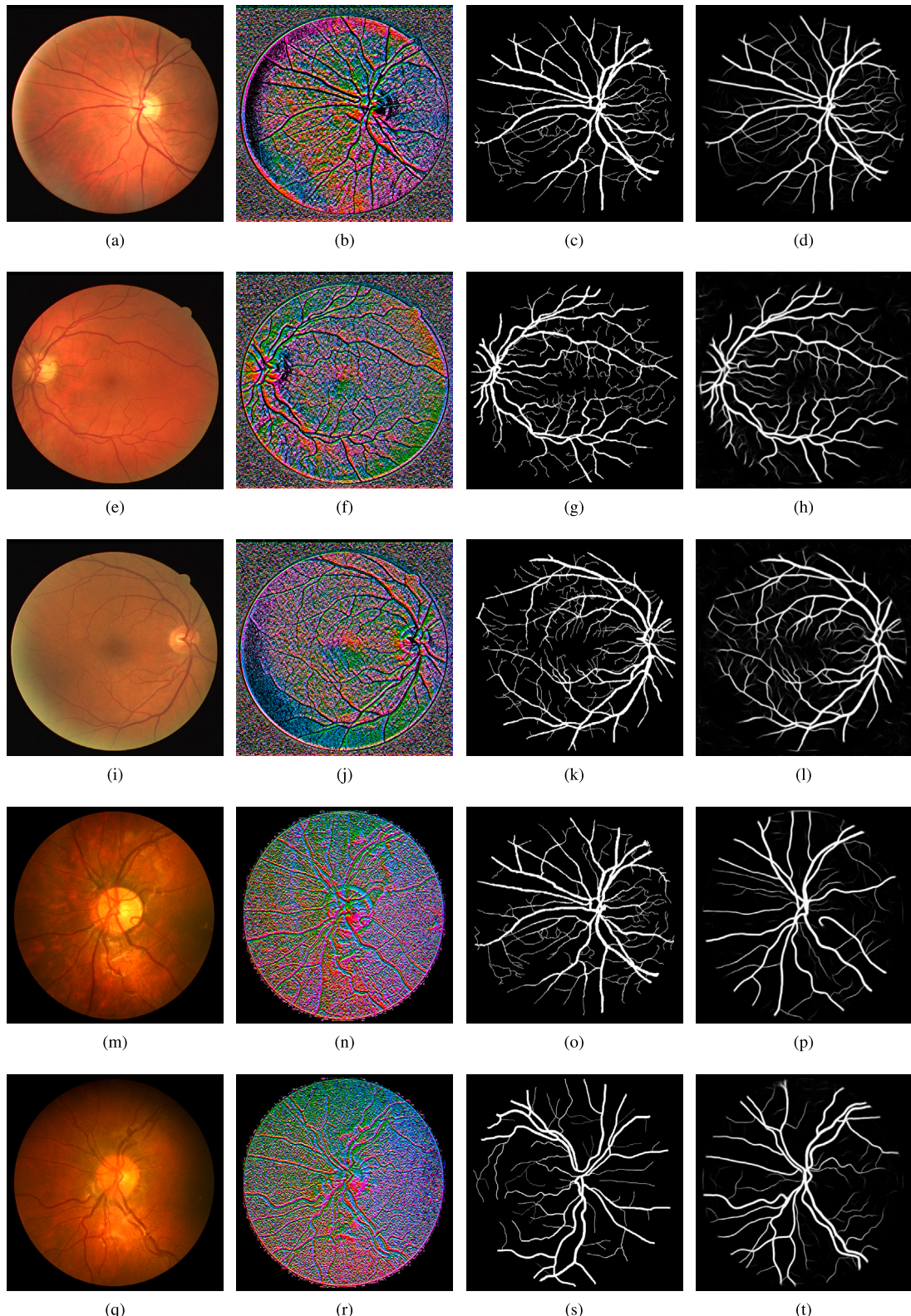


Fig. 7. First row: DRIVE 04_test image, RIOT image, ground truth, extracted using proposed method; Second row: same sequences of row 1 for DRIVE 05_training image; Third row: same sequences of row 1 for STARE image; Fourth row: same sequences of row 1 for CHASE image001; Fifth row: same sequences of row 1 for CHASE image006.

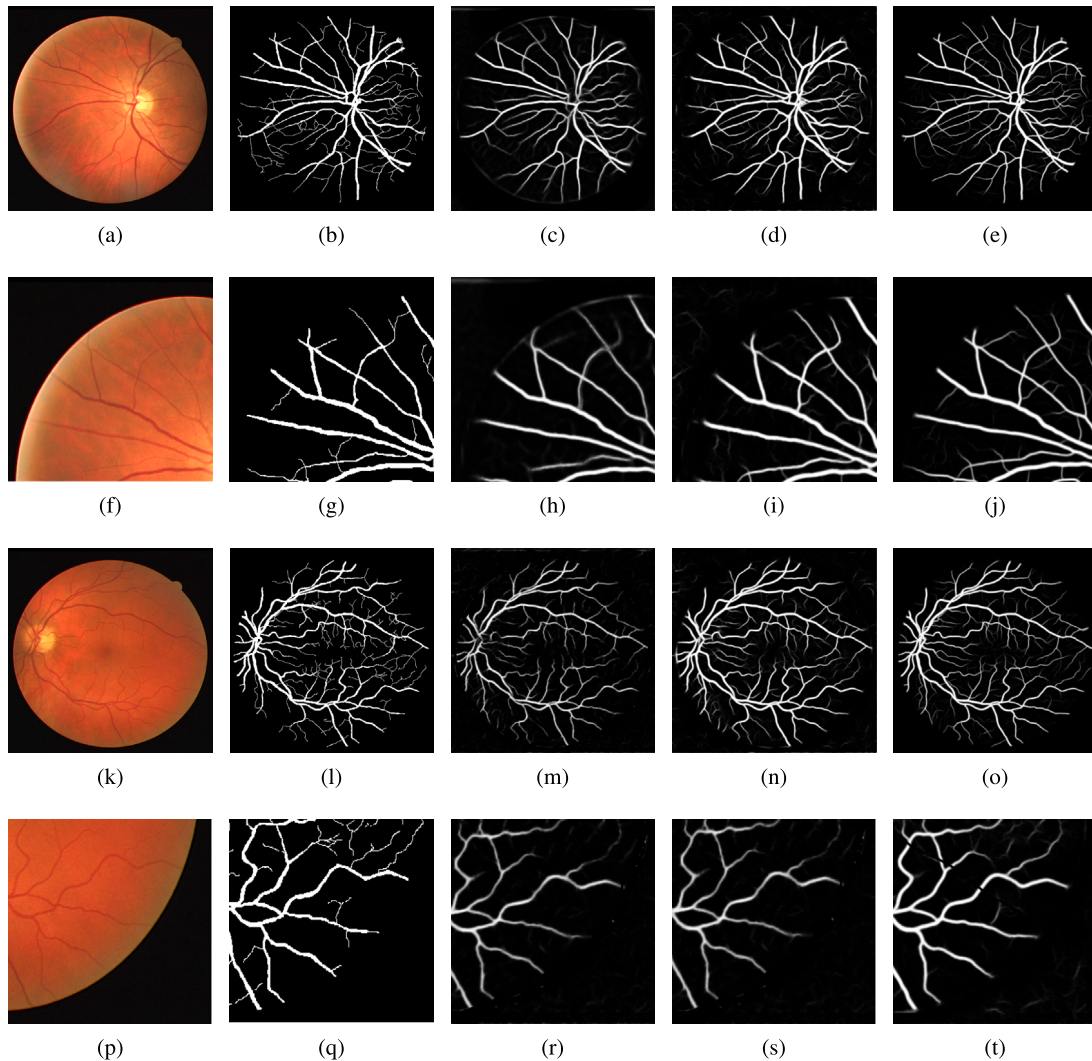


Fig. 8. First row: input DRIVE 04_test image, ground truth, segmented output with IterNet, LIOT and Proposed method; Second row: input DRIVE 04_test clip image, ground truth, segmented output with IterNet, LIOT and proposed method; Third row: input DRIVE 05_training image, ground truth segmented output with IterNet, LIOT and proposed method; Fourth row: input DRIVE 05_training clip image, segmented output with IterNet, LIOT and proposed method;

Table 2
Performance evaluation of the proposed methodology.

Images	Precision	Sensitivity	Specificity	Seg_acc	Dice_Coefficient	F1 score
DRIVE DATASET						
04 test image	0.8358	0.8145	0.9806	0.9627	0.8281	0.825013
05 test image	0.7799	0.8388	0.9762	0.9634	0.821	0.808278
06 test image	0.7671	0.8581	0.9731	0.9615	0.8129	0.810052
Average of 40 images	0.78 ± 0.02	0.82 ± 0.05	0.97 ± 0.017	0.96 ± 0.08	0.82 ± 0.07	0.81 ± 0.015
CHASEDB1 DATASET						
01 test image	0.8752	0.8932	0.9988	0.9982	0.9372	0.884108
05 test image	0.8877	0.9988	0.9962	0.9972	0.9421	0.939979
Average of 28 images	0.87 ± 0.014	0.95 ± 0.045	0.99 ± 0.03	0.99 ± 0.01	0.92 ± 0.015	0.90 ± 0.045
STARE DATASET						
stare 001 image	0.4623	0.5502	0.9331	0.8946	0.511	0.309139
stare 081 image	0.3176	0.5757	0.8722	0.841	0.4179	0.232821
Average of 20 images	0.45 ± 0.023	0.55 ± 0.067	0.89 ± 0.023	0.87 ± 0.034	0.47 ± 0.05	0.35 ± 0.05

Table 3
Comparison of the transforms used for blood vessel segmentation [39] with the proposed model.

Dataset	Method	Sensitivity	Specificity	Accuracy	F1 score	AUC
DRIVE	BaseLine	0.729	0.842	0.828	0.518	0.871
	Census	0.591	0.778	0.755	0.38	0.762
	LIOT	0.752	0.967	0.94	0.761	0.952
	RIOT	0.812	0.982	0.962	0.7902	0.956
CHASEDB1	RIOT+ Edge Feature	0.828	0.988	0.968	0.8105	0.969
	BaseLine	0.633	0.899	0.875	0.477	0.867
	Census	0.781	0.977	0.96	0.778	0.973
	LIOT	0.788	0.977	0.96	0.96	0.978
STARE	RIOT	0.932	0.981	0.972	0.9015	0.982
	RIOT+ Edge Feature	0.955	0.993	0.991	0.9045	0.985
	BaseLine	0.429	0.88	0.833	0.389	0.754
	Census	0.42	0.976	0.918	0.518	0.842
CHASEDB1	LIOT	0.461	0.965	0.912	0.523	0.827
	RIOT	0.533	0.864	0.866	0.402	0.826
	RIOT+ Edge Feature	0.556	0.89	0.874	0.409	0.84

Table 4
Performance evaluation in comparison with other latest models.

Dataset	Method	Sensitivity	Specificity	seg_acc	F1score
DRIVE	IterNet [41]	0.828	0.973	0.954	0.821
	LIOT [39]	0.811	0.974	0.953	0.814
	Proposed	0.828	0.975	0.9608	0.816
CHASEDB1	IterNet [41]	0.633	0.899	0.875	0.477
	LIOT [39]	0.788	0.977	0.96	0.776
	Proposed	0.955	0.99	0.99	0.9
STARE	IterNet [41]	0.429	0.88	0.754	0.373
	LIOT [39]	0.461	0.965	0.912	0.514
	Proposed	0.556	0.89	0.874	0.409

CRediT authorship contribution statement

Chandrakala Kuruba: Conceptualization, Methodology, Writing – original draft, Validation and Writing, Implementation, Writing – review & editing. **N.P. Gopalan:** Problem identification, Supervised the work, Review and editing.

Declaration of competing interest

The authors have no conflict of interest in any manner related to the paper.

Data availability

Data will be made available on request.

Acknowledgments

All authors have read and agreed to the published version of the manuscript. There is no funding received for the proposed work.

References

- [1] S. Ahn, Q.T. Pham, J. Shin, S.J. Song, Future image synthesis for diabetic retinopathy based on the lesion occurrence probability, *Electronics* 10 (6) (2021) 726.
- [2] T.Y. Wong, C. Sabanayagam, Strategies to tackle the global burden of diabetic retinopathy: from epidemiology to artificial intelligence, *Ophthalmologica* 243 (1) (2020) 9–20.
- [3] F. Ghanchi, C. Bailey, U. Chakravarthy, S. Cohen, P. Dodson, J. Gibson, G. Menon, M. Muqit, R. Pilling, J. Olson, et al., Diabetic retinopathy guidelines, London: R. Coll. Ophthalmol. (2012) 9–64.
- [4] S. Demir, P.P. Nawroth, S. Herzig, B. Ekim Üstünel, Emerging targets in type 2 diabetes and diabetic complications, *Adv. Sci.* 8 (18) (2021) 2100275.
- [5] J.L. Morrison, L.A. Hodgson, L.L. Lim, S. Al-Qureshi, Diabetic retinopathy in pregnancy: A review, *Clin. Exp. Ophthalmol.* 44 (4) (2016) 321–334.
- [6] P. Bibiloni, M. González-Hidalgo, S. Massanet, A survey on curvilinear object segmentation in multiple applications, *Pattern Recognit.* 60 (2016) 949–970.
- [7] O. Merveille, B. Naegel, H. Talbot, N. Passat, n D variational restoration of curvilinear structures with prior-based directional regularization, *IEEE Trans. Image Process.* 28 (8) (2019) 3848–3859.
- [8] A. Rehman, M. Harouni, M. Karimi, T. Saba, S.A. Bahaj, M.J. Awan, Microscopic retinal blood vessels detection and segmentation using support vector machine and K-nearest neighbors, *Microsc. Res. Tech.* 85 (5) (2022) 1899–1914.
- [9] M.S. Devi, T. Thenmozhi, Data augmentation for improving proliferative diabetic retinopathy detection in eye fundus images using machine learning techniques, *Elementary Educ.* Online 20 (1) (2022) 5125.
- [10] Y. Zhou, B. Wang, X. He, S. Cui, L. Shao, DR-GAN: conditional generative adversarial network for fine-grained lesion synthesis on diabetic retinopathy images, *IEEE J. Biomed. Health Inf.* (2020).
- [11] A. Mosinska, M. Koziński, P. Fua, Joint segmentation and path classification of curvilinear structures, *IEEE Trans. Pattern Anal. Mach. Intell.* 42 (6) (2019) 1515–1521.
- [12] V. Cherukuri, V.K. Bg, R. Bala, V. Monga, Deep retinal image segmentation with regularization under geometric priors, *IEEE Trans. Image Process.* 29 (2019) 2552–2567.
- [13] S. Dey, A subpixel residual U-net and feature fusion preprocessing for retinal vessel segmentation, in: European Conference on Computer Vision, Springer, 2020, pp. 239–250.
- [14] L. Mou, Y. Zhao, H. Fu, Y. Liu, J. Cheng, Y. Zheng, P. Su, J. Yang, L. Chen, A.F. Frangi, et al., CS2-net: Deep learning segmentation of curvilinear structures in medical imaging, *Med. Image Anal.* 67 (2021) 101874.
- [15] L. Ding, M.H. Bawany, A.E. Kuriyan, R.S. Ramchandran, C.C. Wykoff, G. Sharma, A novel deep learning pipeline for retinal vessel detection in fluorescein angiography, *IEEE Trans. Image Process.* 29 (2020) 6561–6573.
- [16] J. Zhang, Y. Qiao, M.S. Sarabi, M.M. Khansari, J.K. Gahm, A.H. Kashani, Y. Shi, 3D shape modeling and analysis of retinal microvasculature in OCT-angiography images, *IEEE Trans. Med. Imaging* 39 (5) (2019) 1335–1346.
- [17] H. Wu, W. Wang, J. Zhong, B. Lei, Z. Wen, J. Qin, Scs-net: A scale and context sensitive network for retinal vessel segmentation, *Med. Image Anal.* 70 (2021) 102025.
- [18] Z. Shen, H. Fu, J. Shen, L. Shao, Modeling and enhancing low-quality retinal fundus images, *IEEE Trans. Med. Imaging* 40 (3) (2020) 996–1006.
- [19] J. Xie, L. Fang, B. Zhang, J. Chanussot, S. Li, Super resolution guided deep network for land cover classification from remote sensing images, *IEEE Trans. Geosci. Remote Sens.* 60 (2021) 1–12.
- [20] J. Yue, L. Fang, H. Rahmani, P. Ghamisi, Self-supervised learning with adaptive distillation for hyperspectral image classification, *IEEE Trans. Geosci. Remote Sens.* 60 (2021) 1–13.
- [21] J. Staal, M.D. Abràmoff, M. Niemeijer, M.A. Viergever, B. Van Ginneken, Ridge-based vessel segmentation in color images of the retina, *IEEE Trans. Med. Imaging* 23 (4) (2004) 501–509.

- [22] A. Hoover, V. Kouznetsova, M. Goldbaum, Locating blood vessels in retinal images by piecewise threshold probing of a matched filter response, *IEEE Trans. Med. Imaging* 19 (3) (2000) 203–210.
- [23] M.M. Fraz, P. Remagnino, A. Hoppe, B. Uyyanonvara, A.R. Rudnicka, C.G. Owen, S.A. Barman, An ensemble classification-based approach applied to retinal blood vessel segmentation, *IEEE Trans. Biomed. Eng.* 59 (9) (2012) 2538–2548.
- [24] J.S. Bhatti, A. Sehrawat, J. Mishra, I.S. Sidhu, U. Navik, N. Khullar, S. Kumar, G.K. Bhatti, P.H. Reddy, Oxidative stress in the pathophysiology of type 2 diabetes and related complications: Current therapeutics strategies and future perspectives, *Free Radic. Biol. Med.* (2022).
- [25] A. Shanthini, G. Manogaran, G. Vadivu, Background of diabetic retinopathy, in: *Deep Convolutional Neural Network for the Prognosis of Diabetic Retinopathy*, Springer, 2023, pp. 3–17.
- [26] J. Zhang, Y. Cui, W. Jiang, L. Wang, Blood vessel segmentation of retinal images based on neural network, in: *International Conference on Image and Graphics*, Springer, 2015, pp. 11–17.
- [27] D. Maji, A. Santara, P. Mitra, D. Sheet, Ensemble of deep convolutional neural networks for learning to detect retinal vessels in fundus images, 2016, arXiv preprint [arXiv:1603.04833](https://arxiv.org/abs/1603.04833).
- [28] H. Fu, Y. Xu, D.W.K. Wong, J. Liu, Retinal vessel segmentation via deep learning network and fully-connected conditional random fields, in: 2016 IEEE 13th International Symposium on Biomedical Imaging, ISBI, IEEE, 2016, pp. 698–701.
- [29] A. Wu, Z. Xu, M. Gao, M. Buty, D.J. Mollura, Deep vessel tracking: A generalized probabilistic approach via deep learning, in: 2016 IEEE 13th International Symposium on Biomedical Imaging, ISBI, IEEE, 2016, pp. 1363–1367.
- [30] Z. Yao, Z. Zhang, L.-Q. Xu, Convolutional neural network for retinal blood vessel segmentation, in: 2016 9th International Symposium on Computational Intelligence and Design, ISCID, 1, IEEE, 2016, pp. 406–409.
- [31] S. Guo, K. Wang, H. Kang, Y. Zhang, Y. Gao, T. Li, BTS-DSN: Deeply supervised neural network with short connections for retinal vessel segmentation, *Int. J. Med. Inform.* 126 (2019) 105–113.
- [32] Z. Yan, X. Yang, K.-T. Cheng, A three-stage deep learning model for accurate retinal vessel segmentation, *IEEE J. Biomed. Health Inf.* 23 (4) (2018) 1427–1436.
- [33] T.A. Soomro, A.J. Afifi, L. Zheng, S. Soomro, J. Gao, O. Hellwich, M. Paul, Deep learning models for retinal blood vessels segmentation: A review, *IEEE Access* 7 (2019) 71696–71717.
- [34] C. Chen, J.H. Chuah, R. Ali, Y. Wang, Retinal vessel segmentation using deep learning: A review, *IEEE Access* 9 (2021) 111985–112004.
- [35] M. Ciechlewski, M. Kassjański, Computational methods for liver vessel segmentation in medical imaging: A review, *Sensors* 21 (6) (2021) 2027.
- [36] A.A. Abdulsahib, M.A. Mahmoud, M.A. Mohammed, H.H. Rasheed, S.A. Mostafa, M.S. Maashi, Comprehensive review of retinal blood vessel segmentation and classification techniques: intelligent solutions for green computing in medical images, current challenges, open issues, and knowledge gaps in fundus medical images, *Netw. Model. Anal. Health Inform. Bioinform.* 10 (1) (2021) 1–32.
- [37] D. Chen, Y. Ao, S. Liu, Semi-supervised learning method of u-net deep learning network for blood vessel segmentation in retinal images, *Symmetry* 12 (7) (2020) 1067.
- [38] P.M. Samuel, T. Veeramalai, VSSC net: vessel specific skip chain convolutional network for blood vessel segmentation, *Comput. Methods Programs Biomed.* 198 (2021) 105769.
- [39] T. Shi, N. Boutry, Y. Xu, T. Géraud, Local intensity order transformation for robust curvilinear object segmentation, *IEEE Trans. Image Process.* 31 (2022) 2557–2569.
- [40] P. Saranya, S. Prabakaran, R. Kumar, E. Das, Blood vessel segmentation in retinal fundus images for proliferative diabetic retinopathy screening using deep learning, *Vis. Comput.* 38 (3) (2022) 977–992.
- [41] M. Zhu, K. Zeng, G. Lin, Y. Gong, T. Hao, K. Wattanachote, X. Luo, IterNet++: An improved model for retinal image segmentation by curvelet enhancing, guided filtering, offline hard-sample mining, and test-time augmenting, *IET Image Process.* (2022).
- [42] Y. Yang, Z. Wang, J. Liu, K.-T. Cheng, X. Yang, Label refinement with an iterative generative adversarial network for boosting retinal vessel segmentation, 2019, arXiv preprint [arXiv:1912.02589](https://arxiv.org/abs/1912.02589).
- [43] Z. Chen, W. Jin, X. Zeng, L. Xu, Retinal vessel segmentation based on task-driven generative adversarial network, *IET Image Process.* 14 (17) (2020) 4599–4605.
- [44] K. Acharya, D. Ghoshal, Central moment and multinomial based sub image clipped histogram equalization for image enhancement, *Int. J. Image, Graph. Signal Process. (IJGSP)* 13 (1) (2021) 1–12.
- [45] M. Qaid, S. Basah, H. Yazid, M. Safar, M.M. Som, C. Lim, Modelling of retinal images for analysis of diabetic retinopathy severity levels, in: *J. Phys.: Conf. Ser.*, 2071, (1) IOP Publishing, 2021, 012047.
- [46] M.M. Fraz, P. Remagnino, A. Hoppe, B. Uyyanonvara, A.R. Rudnicka, C.G. Owen, S.A. Barman, An ensemble classification-based approach applied to retinal blood vessel segmentation, *IEEE Trans. Biomedical Eng.* (ISSN: 0018-9294) 59 (9) (2012) 2538–2548, <http://dx.doi.org/10.1109/TBME.2012.2205687>.